



EUROPEAN ORGANIZATION FOR NUCLEAR RESEARCH

CERN-LEP-RF/87-25

and

CLIC NOTE 36
March 1987

STUDIES OF RF ACCELERATING STRUCTURES FOR AN ELECTRON LINEAR COLLIDER

J.-P. Boiteux, T. Garvey, G. Geschonke, W. Schnell and I. Wilson

ABSTRACT

Radio-frequency parameters of "crossbar" and "ladder" accelerating structures were measured. These could be an alternative to disk-loaded waveguides in high energy linear colliders.

Geneva, Switzerland
March 1987

1. Introduction

For electron-positron colliding linacs a scheme has been proposed¹⁾ where travelling-wave accelerating cavities working at 29 GHz are used. These cavities should have relatively high group velocities v_g for two main reasons: a) the attenuation constant for energy per section length α has been chosen to be 0.5: therefore in order to avoid an excessive number of RF feed points v_g should be large; b) since the RF pulse length is only 330 RF cycles, the passband of the structure should be large to minimize deformations of the travelling wave.

The disc-loaded circular waveguides used for example at SLAC²⁾ and the LEP injector linac LIL³⁾ have only a small group velocity of a few per cent of the speed of light. This can be increased by opening up the beam aperture, at the expense of a loss in shunt impedance. Therefore alternative structures might be of interest. Brass models of several structures operating at frequencies between 1 and 2 GHz were built and their radio-frequency properties measured. For simplicity all these structures were designed for $\pi/2$ phaseshift per cell where in general the group velocity has a maximum.

2. Measurement of shunt impedance

Shunt impedances of these structures were measured on the standing wave models using a perturbation method by moving a metal bead along the beam axis. The phase changes between a quartz stable synthesizer (tuned to the cavities' unperturbed frequency) and the cavities were measured as a function of the bead's position. This yields the spatial E-field distribution. Through integration of the accelerating fields one obtains directly the shunt impedance per unit length R' ; in order to obtain the $r' = R'/Q$ the Q-values of the cavities have to be measured separately. R' and r' are effective impedances, i.e. the effect of time variation of the fields during the passage of particles travelling with the speed of light is taken into account. Since the perturbation measurement is only sensitive to the absolute value and not the direction of the E-fields, the relative phases between adjacent cells (0° or 180°) are measured separately and then transit time effects are taken into account by multiplying the measured spatial field distribution with a suitable sine or cosine function before integration.

The R' and r' for travelling wave operation is then twice that measured on the standing wave models.

3. Crossbar cylinder structure

Two models of this structure were built. They consist of a brass cylinder into which brass bars with beamholes are soft-soldered, adjacent bars being perpendicular to each other.

One version was short with only two gaps and the other had eight gaps. The short one was used to determine the correct dimensions for synchronism between particles and gap fields by adjustment of the cylinder diameter. The eight-gap model was built using these dimensions. Both structures were terminated with flat plates in the centres of the first and last bars. The two-gap model is shown in Figs. 1 and 2, the eight-gap version in Fig. 3.

The measured standing-wave values in the $\pi/2$ -mode for frequency, unloaded Q , effective shunt impedance per unit length R' and $r' = R'/Q$ are given in the first two lines of Table 1. The dispersion diagram measured on the eight-gap structure is shown in Fig. 4. 0-mode and $\pi/2$ -mode frequencies are identical to those found on the two-gap structure.

Fig. 5 shows the field distributions for all eight resonances measured in the lowest passband. Plotted here are the measured phase changes $\Delta\phi$; the electric fields E are given by $E \sim \sqrt{\Delta\phi}$. The arrows indicate the relative orientations of the electric fields at one particular moment.

4. Crossbar disc structure

Another crossbar structure was built where the bars are milled out of solid discs which were clamped together for the model measurements. It was hoped that this design would have a higher Q because of a lower current density on the bars. Figs. 6 and 7 show the mechanical design.

Two versions with different beam hole diameters were measured. The results are shown in lines 3 and 4 of Table 1.

5. Ridged waveguide with parallel bars ('ladder structure')

Contrary to the previous structures this one is of the forward wave type. It consists essentially of a rectangular waveguide, longitudinally loaded with a "ladder" type structure. Its layout is shown in Figs. 8 and 9. The resonant frequency was adjusted for synchronism between particles and RF wave by increasing the height of the windows.

The results of the measurements are given in the last line of Table 1. The field profile for the $\pi/2$ mode, for which the structure has been made, is shown in Fig. 10. Fig. 11 shows the dispersion diagram.

6. Comparison with pillbox

A cylindrical pillbox was measured which had a diameter of 160.5 mm, a length of 105 mm and consisted of the same brass material as the accelerating structures. The $r' = R'/Q$ measurement for the E_{010} -mode agreed with the theoretical value to within 3%. The Q values were however lower than expected for the given conductivity of 28% of the standard copper conductivity. The unloaded Q for the E_{010} -mode was only 66% of the theoretical value, while that for the H_{011} -mode was 72%. This is believed to be due to surface roughness, bad contacts and perhaps a lower conductivity of the brass material used.

7. Scaling results

The measured values were scaled to 29 GHz for travelling wave copper cavities. The results are shown in Table 2 on the left. These values are, however, certainly pessimistic: real structures would be much longer than the models. This increases the Q-value because the effect of the end plates is reduced. Also electrical contacts should be better than in the models. The Q values are therefore likely to be higher, at least 85% (say) of the theoretical values instead of the $\sim 70\%$ measured on the pillbox.

A structure operating at a different phase shift per cell can give higher shunt impedance, e.g. a 10% increase in R' is quoted in ref. 2) for using $2\pi/3$ - instead of $\pi/2$ -mode. According to the data shown in ref. 2), the Q value also increases; therefore the r' should stay roughly the same.

8. Comparison with disc loaded waveguides

Disk loaded waveguides (DLW) as used in SLAC and LIL have low group velocities of 1-2% of c . v_g can be increased by increasing the beam hole diameter. This is also very advantageous for stability against transverse wake field effects, though at the expense of Q , R' and r' .

The shunt impedance of the best crossbar structure, 160 M Ω /m, could be achieved with a DLW structure with a much bigger beam hole diameter of 0.27λ as compared to only 0.1λ of the crossbar structure. The r' of this DLW is, however, only 50% of that of the crossbar structure and the group velocity is 2.5% as compared to 27%.

The type of structure to be preferred will strongly depend on the necessary beam hole size. DLWs appear to give good R' with big beam holes but it seems difficult to reach group velocities as high as with the structures investigated.

None of the structures used have been optimized so far. They all have high group velocities of $> 25\%$ of the speed of light which is perhaps not needed. Therefore a higher shunt impedance and higher Q can certainly be achieved by varying geometry parameters.

The "optimistic" parameters on the right of Table 2 have been obtained by taking a $2\pi/3$ structure and an increase in Q from 70% to 85%.

9. References

- 1) W. Schnell, Radio-frequency acceleration for linear colliders, CERN-LEP-RF/86-27.
- 2) G.A. Loew et al., in chapter 6 of "The Stanford Two Mile Accelerator", ed. by R.B. Neal (W.A. Benjamin, New York 1968).
- 3) G. Biennu, J.-C. Bourdon, P. Brunet and J. Rodier, Accelerating structure developments for the LEP injector linacs (LIL), in Proc. 1984 Linac Conf., GSI 84-11, 463 (1984).

Table 1 Measured parameters on brass models

	beam hole diameter [in units of wave- length λ]	frequency of $\pi/2$ -mode [MHz]	Q (unloaded)	$r' = R'/Q$ [k Ω/m] (for standing wave)
crossbar cylinder two gaps	0.100	1099.6	4953	1.13
crossbar cylinder eight gaps	0.100	1099.8	5115	1.20
crossbar disk (bigger beam hole)	0.168	1257.7	5200	1.01
crossbar disk (smaller beam hole)	0.114	1249.5	5060	1.15
ridged waveguide with parallel bars	0.15	1429.9	4800	0.96

Table 2 RF parameters scaled to 29 GHz

		Scaled to 29 GHz copper structure					Optimistic values at 29 GHz			
	beam hole diameter [in units of wave- length λ]	group velo- city v_g/c	$r' = R'/Q$ for travel- ing wave [$k\Omega/m$]	Q_0	R' [$M\Omega/m$]	$r' = R'/Q$ (different mode)	Q_c	R' [$M\Omega/m$]		
crossbar cylinder eight gaps	0.100	27%	63.5	1882	119	63.5	2503	159		
crossbar disk (bigger beam hole)	0.168	25%	46.4	2046	95	46.4	2721	126		
crossbar disk (smaller beam hole)	0.114	25%	53.5	1985	106	53.5	2640	140		
ridged waveguide with parallel bars	0.15	29%	38.9	2014	78	38.9	2679	104		

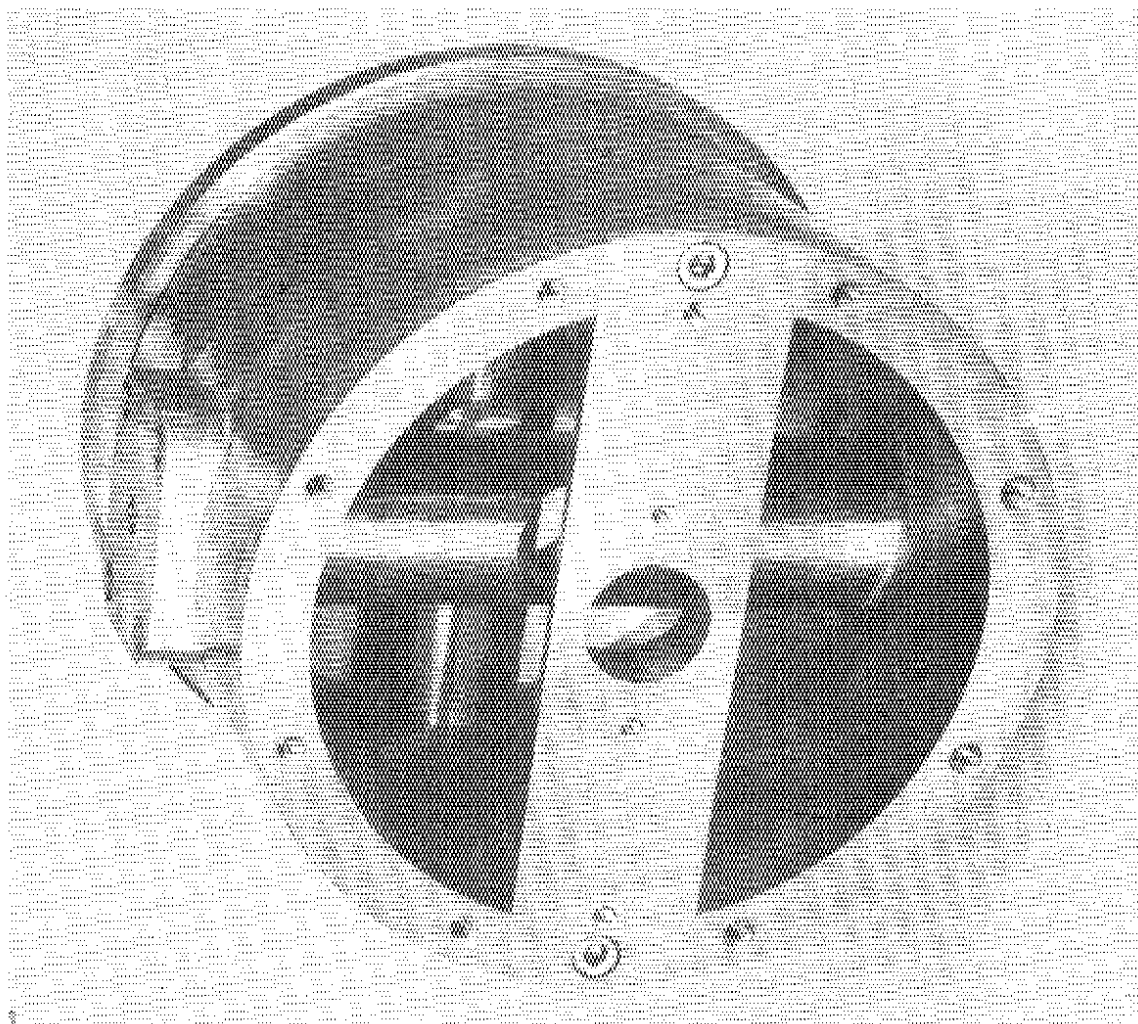


Fig. 2. Photo of two-gap crossbar cylinder structure

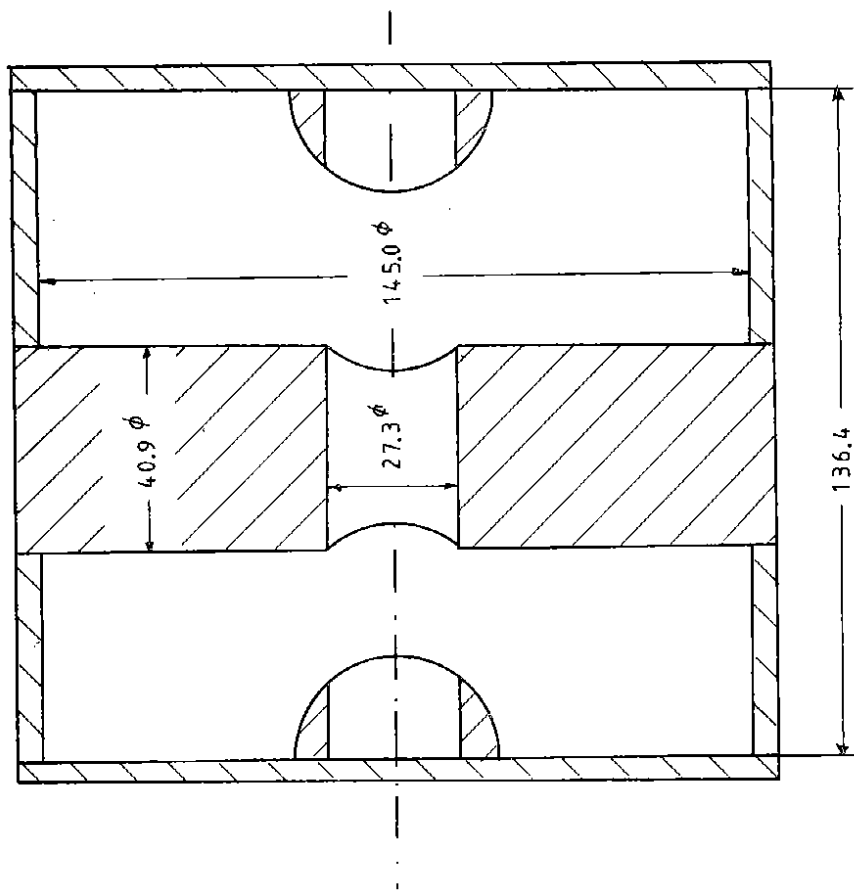


Fig. 1. Dimensions of crossbar cylinder structure

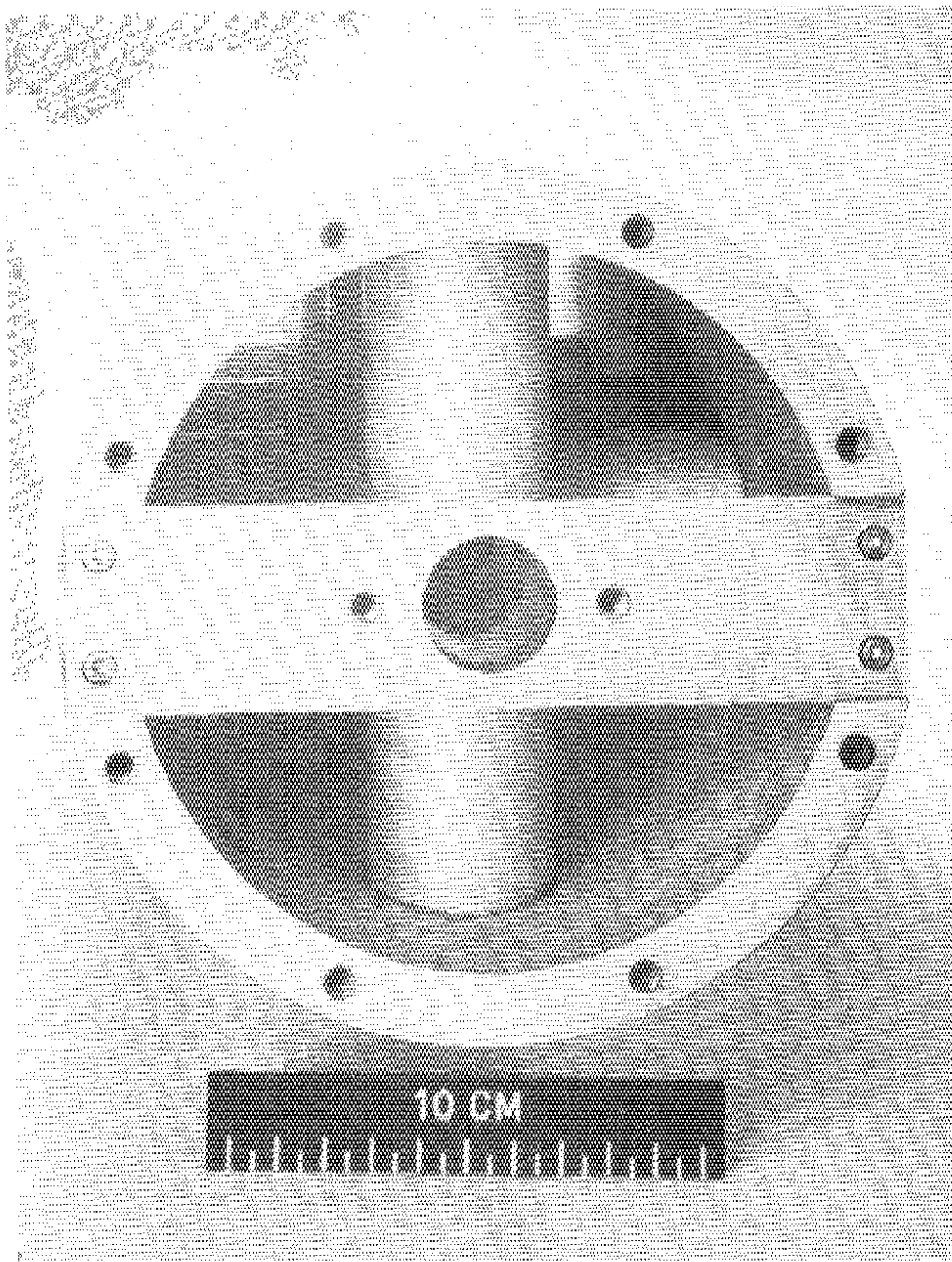


Fig. 3. Eight-gap crossbar cylinder structure

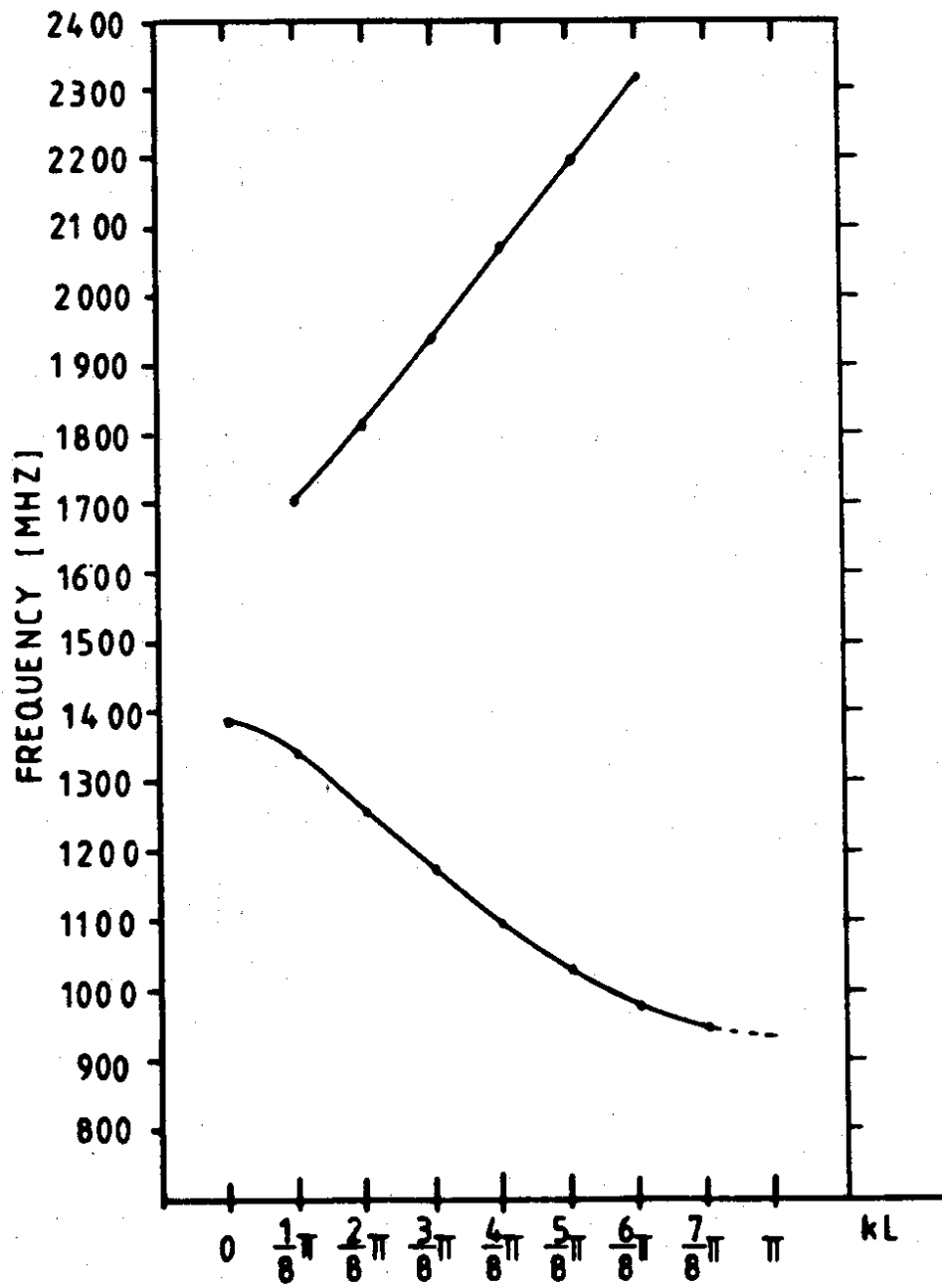


Fig. 4. Dispersion of eight-cell crossbar cylinder structure

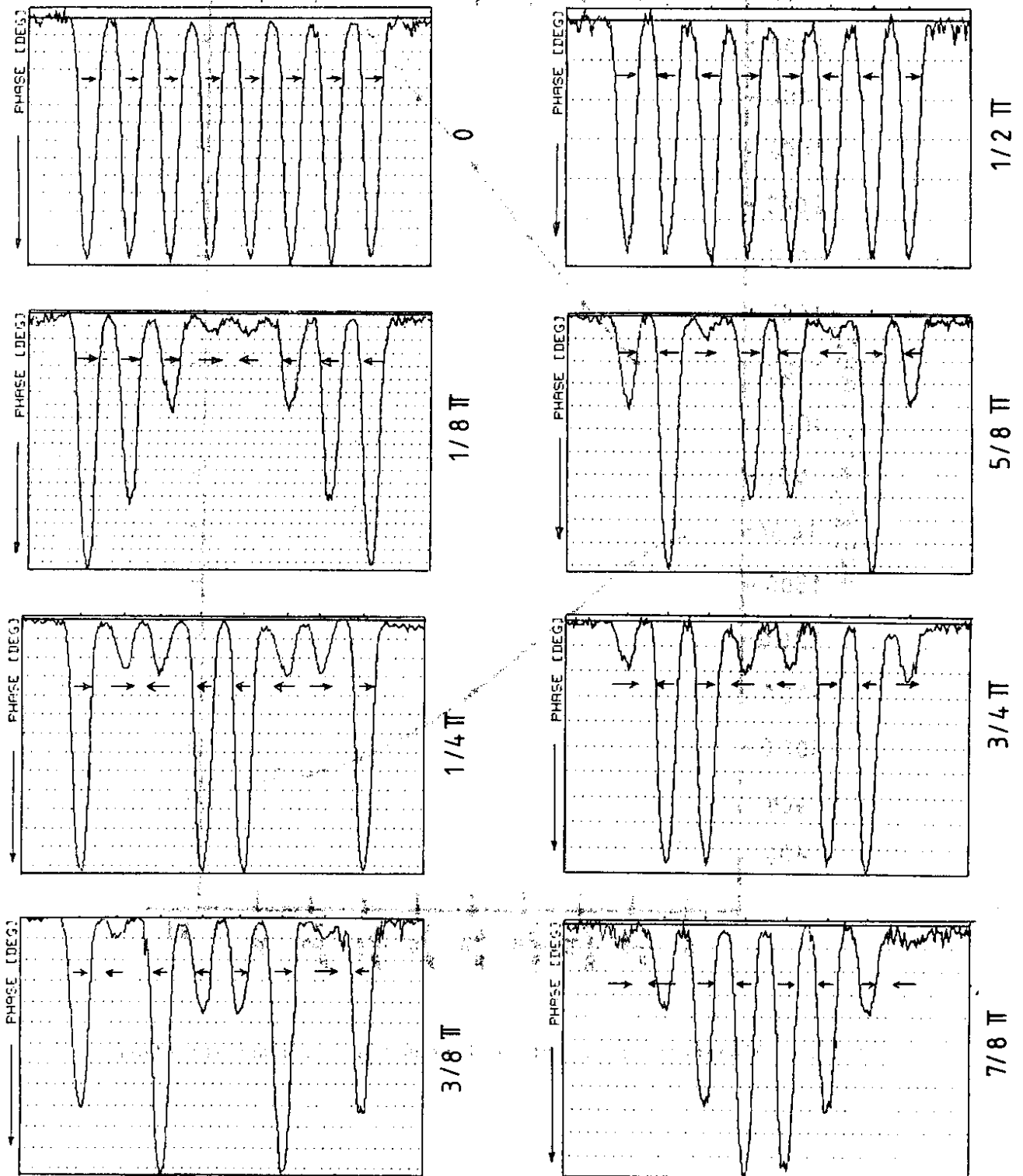


Fig. 5. E-field distributions in the eight gaps of the crossbar cylinder structure for the lowest passband. The phase measured as a function of position is proportional to E^2 .

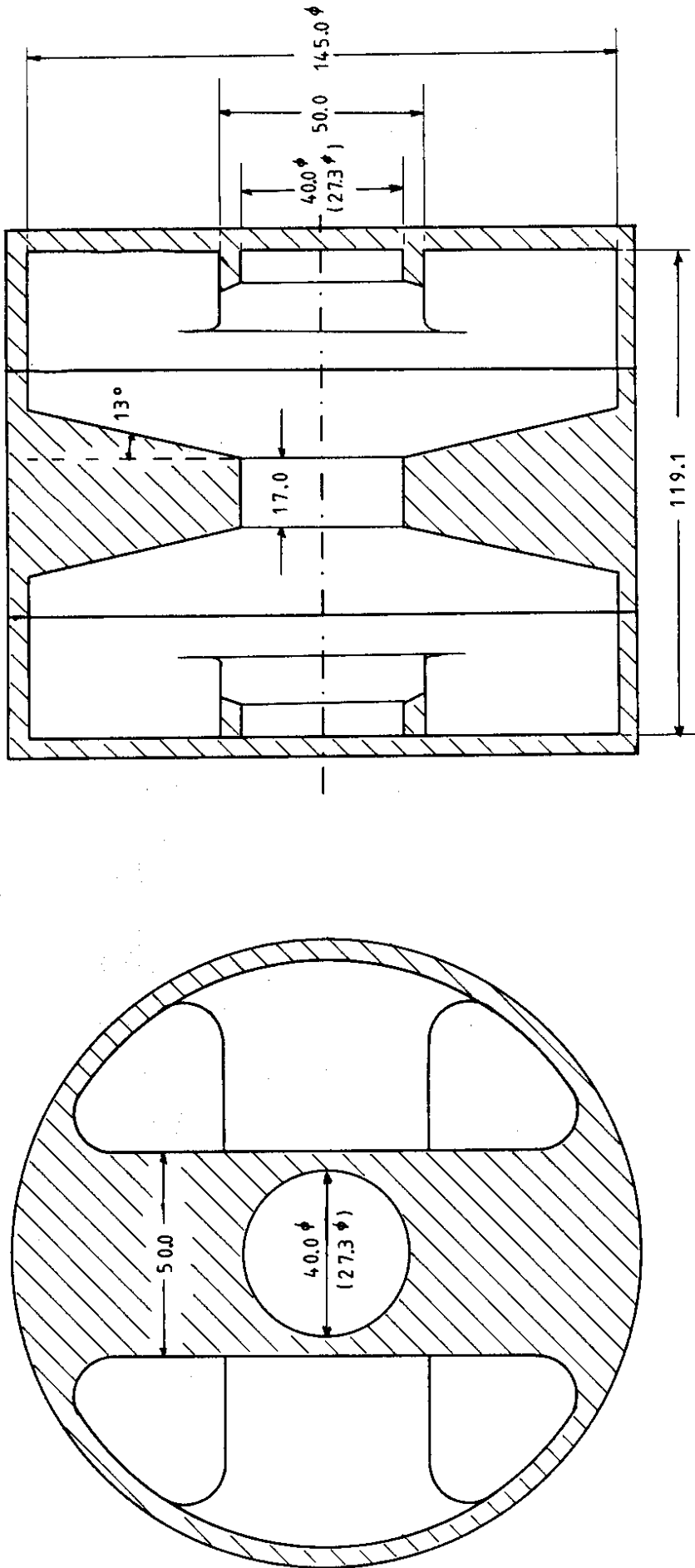


Fig. 6. Crossbar disk structure

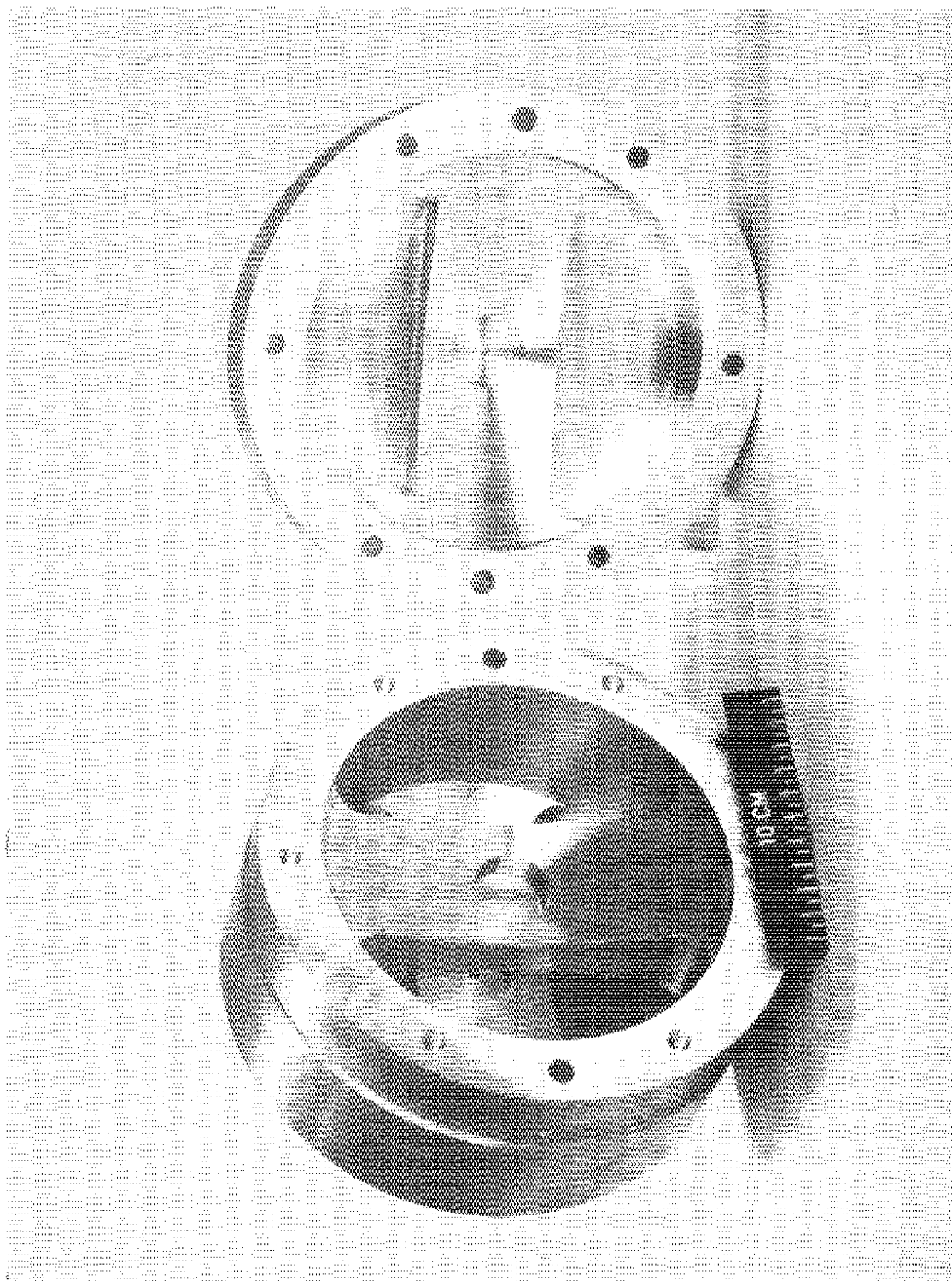


Fig. 7. Crossbar disk structure

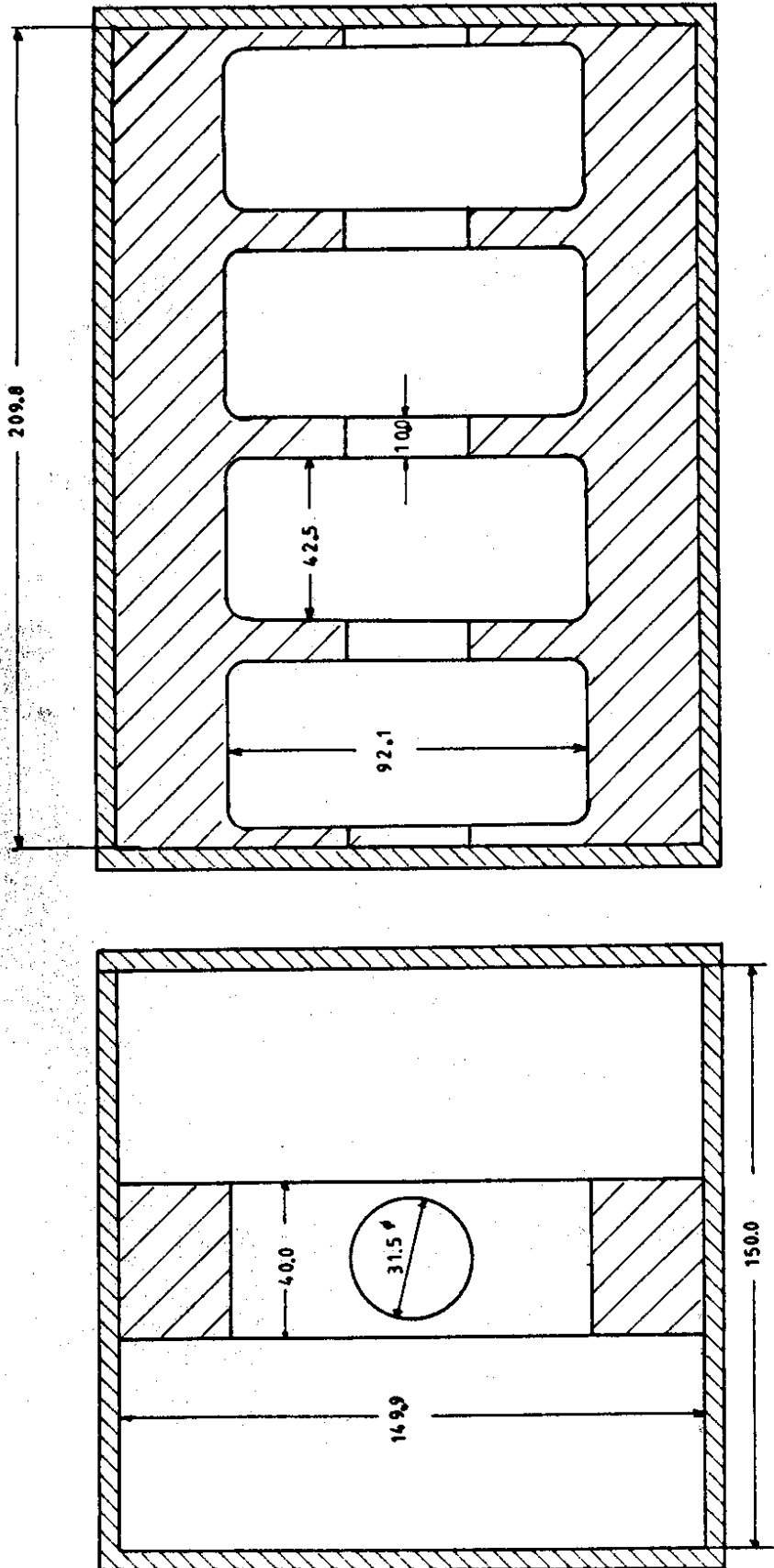


Fig. 8. Ridged waveguide with parallel bars "ladder structure"

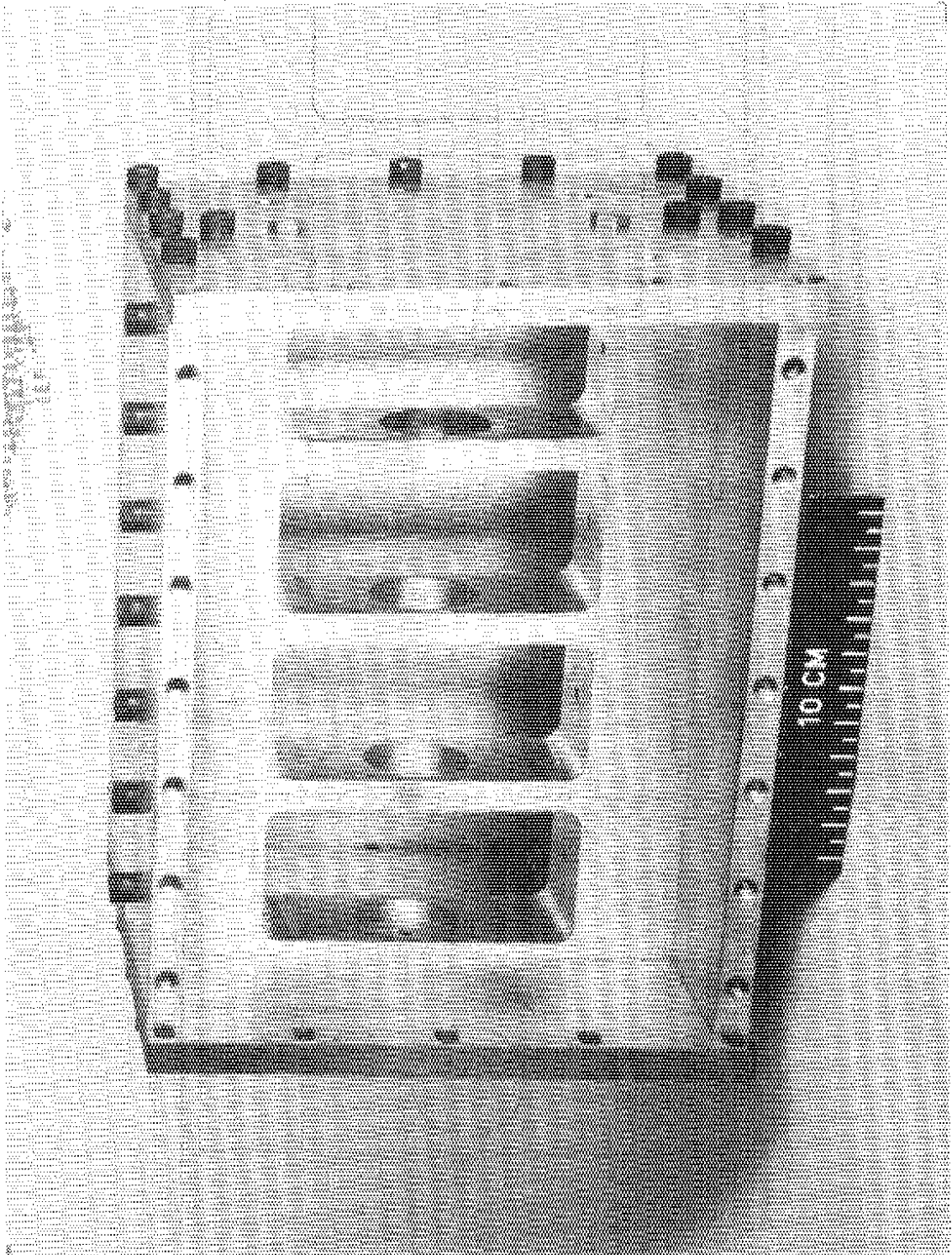


Fig. 9. "Ladder structure"

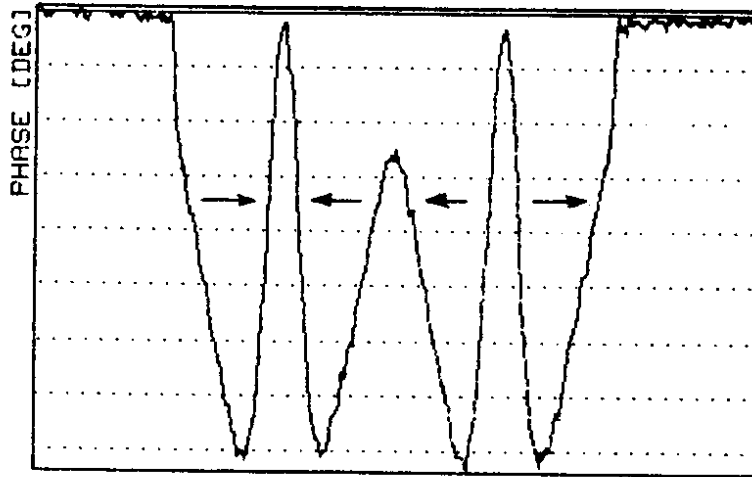


Fig. 10. Field distribution (Phase $\propto E^2$) in the four gaps of the "ladder" structure

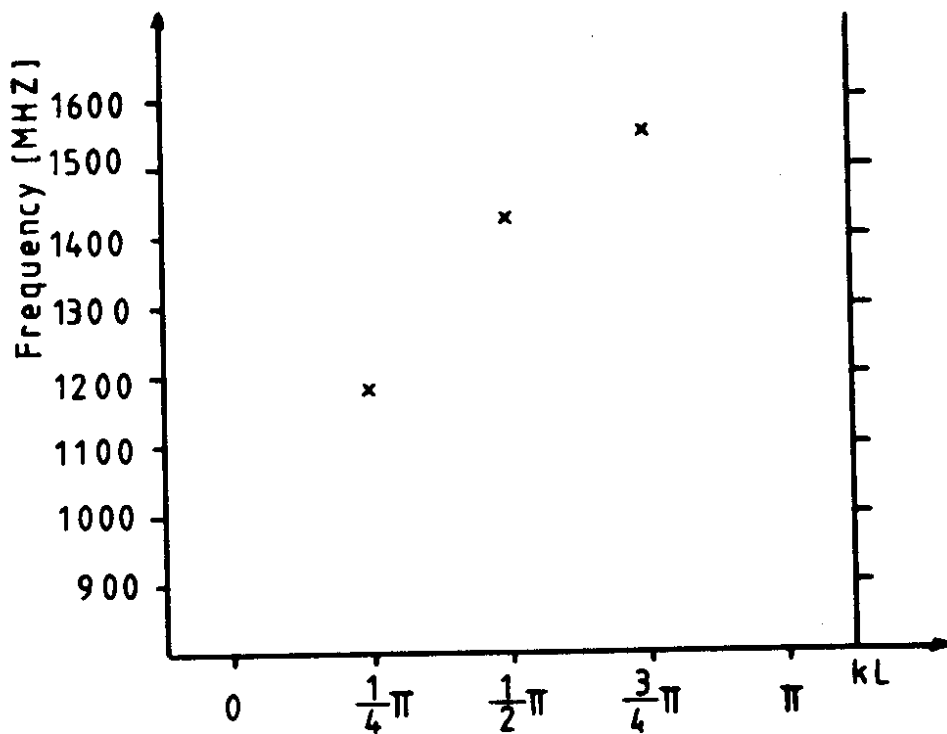


Fig. 11. Dispersion of ladder structure